

DNA Molecular Motor Driven Micromechanical Cantilever Arrays

Wenmiao Shu,[†] Dongsheng Liu,^{†,‡} Moyu Watari,[§] Christian K. Riener,[§]
Torsten Strunz,[§] Mark E. Welland,[†] Shankar Balasubramanian,[‡] and
Rachel A. McKendry^{*,§}

Contribution from The Nanoscience Centre, University of Cambridge,
11 J. J. Thomson Avenue, Cambridge CB3 0FF, United Kingdom, Department of Chemistry,
University of Cambridge, Lensfield Road, Cambridge CB2 1EW, United Kingdom, and
London Centre for Nanotechnology and Department of Medicine, University College London,
5 University Street, London WC1E 6JJ, United Kingdom

Received August 10, 2005; E-mail: R.A.McKendry@ucl.ac.uk

Abstract: The unique ability of living systems to translate biochemical reactions into mechanical work has inspired the design of synthetic DNA motors which generate nanoscale motion via controlled conformational change. However, while Nature has evolved intricate mechanisms to convert molecular shape change into specific micrometer-scale mechanical cellular responses, the integration of artificial DNA motors with mechanical devices presents a major challenge. Here we report the direct integration between an ensemble of DNA motors and an array of microfabricated silicon cantilevers. The forces exerted by the precise duplex to nonclassical i-motif conformational change were probed via differential measurements using an in-situ reference cantilever coated with a nonspecific sequence of DNA. Fueled by the addition of protons, the *open to close* stroke of the motor induced 32 ± 3 mN/m compressive surface stress, which corresponds to a single motor force of approximately 11 pN/m, an order of magnitude larger than previous classical hybridization studies. Furthermore, the surface-tethered conformational change was found to be highly reversible, in contrast to classical DNA motors which typically suffer rapid system poisoning. The direction and amplitude of motor-induced cantilever motion was tuneable via control of buffer pH and ionic strength, indicating that electrostatic forces play an important role in stress generation. Hybrid devices which directly harness the multiple accessible conformational states of dynamic oligonucleotides and aptamers, translating biochemical energy into micromechanical work, present a radical new approach to the construction of “smart” nanoscale machinery and mechano-biosensors.

Introduction

Artificial oligonucleotide motors which reversibly interconvert between two thermodynamically well-defined conformations can generate rotary¹ motion or linear *extension/contractile* movement.^{2–7} The repertoire of DNA conformations which have been exploited in the homogeneous solution-phase motor studies extends from the classical double-helix to more unusual nonclassical, multistranded structures, including the four-stranded i-motif. However, to date the integration of artificial motors with current microscale technology presents a major challenge, so the majority of motor studies have been confined to the homogeneous

solution phase.^{1–4} To harness the forces exerted by molecular machines, a conformationally “active” motor must be tethered to a surface, thus requiring highly optimized surface chemistry.^{6,7} Subtle changes in molecular shape must then be transduced into a measurable mechanical output signal. While physical tools such as optical tweezers⁸ and the atomic force microscope⁹ have the sensitivity to probe the nanomechanics of single oligonucleotides, these measurements occur under an applied load. Conversely, recent experiments have shown when an ensemble of DNA molecules hybridize onto one surface of a microfabricated cantilever, in-plane surface stress forces induce micromechanical bending motion of the cantilever beam.^{10–14} This novel nanomechanical transduction mechanism integrates “bottom up”

* Corresponding author.

[†] The Nanoscience Centre, University of Cambridge.

[‡] Department of Chemistry, University of Cambridge.

[§] University College London.

- (1) Mao, C. D.; Sun, W. Q.; Shen, Z. Y.; Seeman, N. C. *Nature* **1999**, *397*, 144–146.
- (2) Yurke, B.; Turberfield, A. J.; Mills, A. P., Jr.; Simmel, F. C.; Neunmann, J. L. *Nature* **2000**, *406*, 605–608.
- (3) Alberti, P.; Mergny, J. L. *Proc. Natl. Acad. Sci. U.S.A.* **2003**, *100*, 1569–1573.
- (4) Liu, D. S.; Balasubramanian, S. *Angew. Chem., Int. Ed.* **2003**, *42*, 5734–5736.
- (5) Turberfield, A. J.; Mitchell, J. C.; Yurke, B.; Mills, A. P.; Blakey, M. I.; Simmel, F. C. *Phys. Rev. Lett.* **2003**, *90*, 118102.1–118102.4.

- (6) Sherman, W. B.; Seeman, N. C. *Nano Lett.* **2004**, *4*, 1203–1207.
- (7) Shin, J. S.; Pierce, N. A. *J. Am. Chem. Soc.* **2004**, *126*, 10834–10835.
- (8) Bustamante, C.; Marko, J. F.; Smith, S. B.; Siggia, E. D. *Science* **1994**, *265*, 1599–1600.
- (9) Strunz, T.; Oroszlan, K.; Schafer, R.; Guntherodt, H.-J. *Proc. Natl. Acad. Sci. U.S.A.* **1999**, *96*, 11277–11282.
- (10) Fritz, J.; Baller, M. K.; Lang, H. P.; Rothuizen, H.; Vettiger, P.; Meyer, E.; Guntherodt, H. J.; Gerber, C.; Gimzewski, J. K. *Science* **2000**, *288*, 316–318.
- (11) Wu, G. H.; Ji, H. F.; Hansen, K.; Thundat, T.; Datar, R.; Cote, R.; Hagan, M. F.; Chakraborty, A. K.; Majumdar, A. *Proc. Natl. Acad. Sci. U.S.A.* **2001**, *98*, 1560–1564.

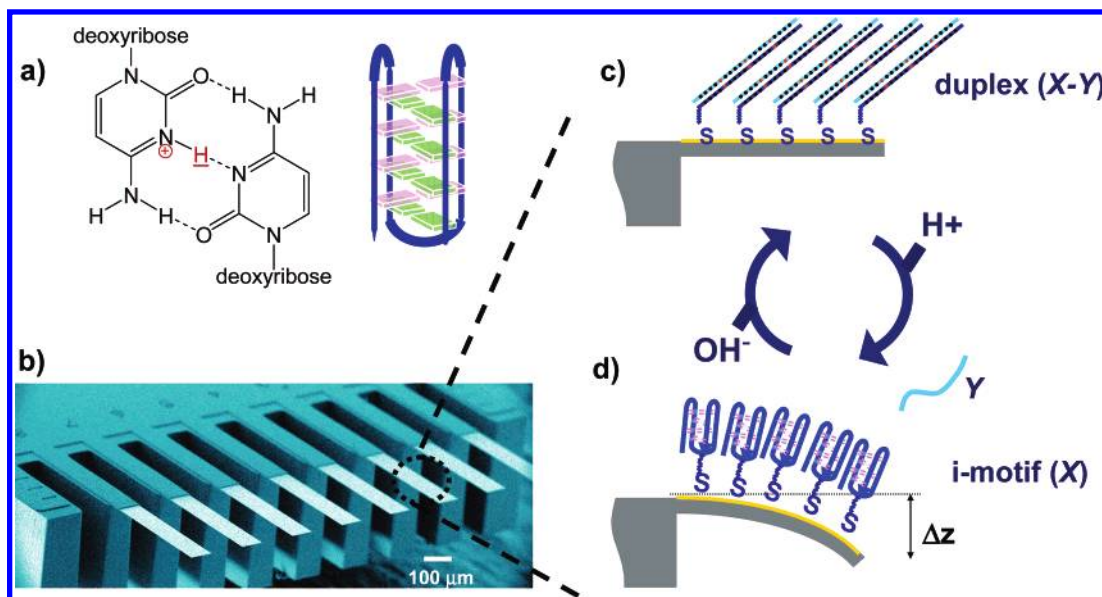


Figure 1. Harnessing duplex to i-motif conformational changes on a micromechanical cantilever array. (a) Chemical structure of a $C^+ : C$ base pair on strand **X** at pH 5.0 to show the three hydrogen bonds formed between a single pair of hemiprotonated cytosine bases and a schematic diagram to show the intramolecular interdigitation of strand **X** to form the i-motif. (b) Scanning Electron Microscope image of an array of eight rectangular silicon cantilevers. (c) Schematic diagram to show a cantilever functionalized on one-side with a thin film of gold and a monolayer of thiolated **X**. At pH > 6.7 hybridization of surface-tethered **X** to strand **Y** in solution ($1 \mu\text{M}$) forms the duplex structure. (d) At pH 5.0, **X** forms the self-folded i-motif and induces repulsive in-plane surface forces (compressive surface stress) which cause the cantilever to bend downward, Δz . Strand **Y** is shown to be present in free solution in a random coil conformation.

molecular design with “top down” microfabrication and does not require applied loads or fluorescent tags. Classical hybridization between probe DNA tethered to the cantilever and target DNA in solution can sequence-specifically detect DNA with single base mismatch sensitivity.^{10–14} Cantilever sensor arrays have attracted much attention as a “label-free” biosensor, but they also offer a unique way to directly probe and indeed harness the surface forces exerted by dynamic biomolecules which can undergo reversible conformational changes. Here we report the direct interface between DNA motors and an array of microfabricated silicon cantilevers and probe the reversible mechanical forces exerted by the precise duplex to i-motif DNA conformational change.

In contrast to polymers¹⁵ and rotaxanes,¹⁶ biomolecular motors offer significant advantages by virtue of the highly specific molecular recognition reactions which have evolved to occur under mild, aqueous conditions. Furthermore, custom synthesis of oligonucleotides offers precise control of base sequence, length, and orientation, giving rise to tuneable physical and chemical properties. Both classical^{1,2} and nonclassical, multistranded DNA structures have been exploited as molecular motors in the homogeneous solution phase.^{3,4} We recently reported a novel motor based on the conversion of a two-stranded duplex to the nonclassical, four-stranded i-motif DNA, triggered by pH.⁴ In contrast to classical DNA motors, which typically suffer system poisoning due to the accumulation of

duplex DNA,^{1,2} this proton-fueled i-motif conformational change was found to be highly reversible in solution and inspired the direct measurement of the nanomechanical forces exerted by surface-tethered motors reported herein.

The proton-fueled DNA motor is illustrated in Figure 1 and has only two components; the first is the cytosine-rich, single-stranded 21 mer oligonucleotide **X**, which contains four stretches of CCC. To tether the motor to a gold surface, the 5' end was tailored with an alkanethiol linker (**X**: $\text{HSC}_6\text{H}_{12}\text{-5'-(CCC AAT CCC AAT CCC AAT CCC)-3'}$). The second component of the molecular machine is the duplex forming strand **Y**, a nonthiolated single-stranded 21 mer, which is present in solution (**Y**: $3'\text{-GTG ATT GGG ATT TGG ATT GTG-5'}$). It was necessary to engineer three base mismatches in strand **Y** (underlined bases) in order to prevent the formation of intramolecular G-quadruplex and to moderate the melting temperature of the **X–Y** duplex, enabling reversible cyclic operation of the nanomachine.⁴ Solution-phase pH titration measurements of the i-motif¹⁷ show a sharp transition at $\text{p}K_a$ 6.5, and thus, the reversible DNA nanomachine can be triggered by pH change.⁴ Under acidic conditions (pH 5.0), intramolecular noncanonical base pair interactions between a protonated and an unprotonated cytosine residue on strand **X** (i.e., a $C^+ : C$ base pair) interdigitate to form an i-motif conformation (Figure 1a). This structure is defined as the *closed* form of the molecular machine. In this state strand **Y** adopts a random coil conformation in solution. In contrast, at pH > 6.5 the cytosine bases become nonprotonated and thus **X** unfolds and hybridizes with strand **Y** in solution, forming the extended double helix, the *open* form of the motor. Circular dichroism¹⁸ (CD) and UV melting studies were used to calculate⁴ the $\Delta\Delta G$ associated with the intercon-

(12) McKendry, R. A.; Zhang, J.; Arntz, Y.; Strunz, T.; Hegner, M.; Lang, H. P.; Baller, M. K.; Certa, U.; Meyer, E.; Güntherodt, H.-J.; Gerber, Ch. *Proc. Natl. Acad. Sci. U.S.A.* **2002**, *99*, 9783–9788.

(13) Fritz, J.; Cooper, E. B.; Gaudet, S.; Sorger, P. K.; Manalis, S. R. *Proc. Natl. Acad. Sci. U.S.A.* **2002**, *99*, 14142–14146.

(14) Mukhopadhyay, R.; Lorentzen, M.; Kjems, J.; Besenbacher, F. *Langmuir* **2005**, *21*, 8400–8408.

(15) Lahav, M.; Durkan, C.; Gabai, R.; Katz, E.; Willner, I.; Welland, M. E. *Angew. Chem., Int. Ed.* **2001**, *113*, 4219–4221.

(16) Huang, T. J.; Brough, B.; Ho, C. M.; Liu, Y.; Flood, A. H.; Bonvallet, P. A.; Tseng, H. R.; Stoddart, J. F.; Baller, M.; Magonov, S. *Appl. Phys. Lett.* **2004**, *22*, 5391–5393.

(17) Leroy, J. L.; Gehring, K.; Kettani, A.; Gueron, M. *Biochemistry* **1993**, *32*, 6019–6031.

(18) Berova, N.; Nakanishi, K.; Woody, R. W. *Circular Dichroism: Principles and Application*, 2nd ed.; John Wiley and Sons: New York, 2000; pp 707–727.

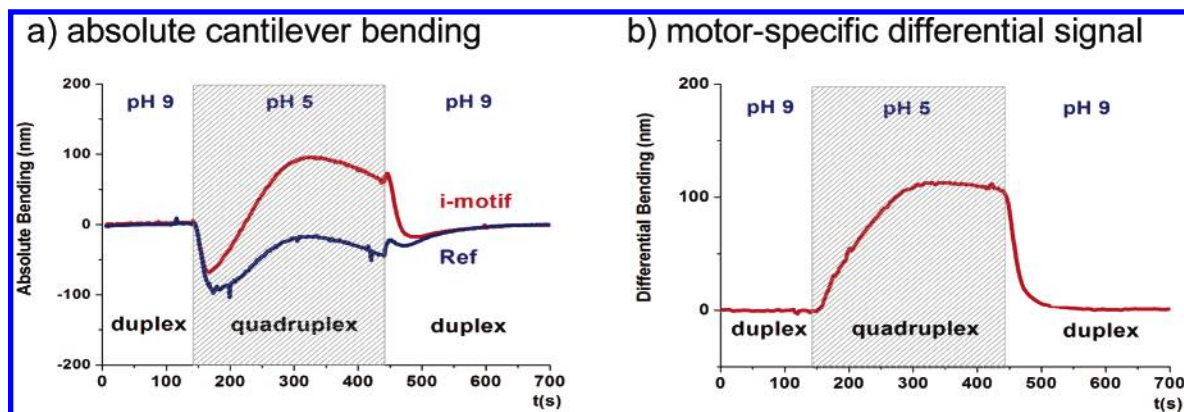


Figure 2. Translating duplex to i-motif molecular conformational changes directly into micromechanical cantilever bending motion. (a) Absolute bending signal of an **X**-coated cantilever (shown in red) and an in-situ **ref**-coated cantilever (shown in blue). A positive absolute bending signal corresponds to a compressive surface stress (i.e. the cantilever bends away from the gold surface (as shown in Figure 1d)), whereas a negative absolute differential bending signal correlates to tensile stress. The shaded area corresponds to the injection of i-motif-forming pH 5.0 buffer. (b) Differential bending signal (**X** – **ref**) reveals the motor-specific induced cantilever surface stress.

version between the *open* and *closed* states in solution of -11.2 kcal/mol and a theoretical extension force⁴ of approximately 16 pN.

To directly probe the forces exerted by the motor, **X** was immobilized onto one side of a gold-coated micromechanical cantilever. Each silicon cantilever measured $500\ \mu\text{m}$ in length, $100\ \mu\text{m}$ in width, and $1\ \mu\text{m}$ in thickness (Figure 1b). These dimensions give rise to a small spring constant of $0.02\ \text{N/m}$, with a resonant frequency of $\sim 4\ \text{kHz}$ in air and a correspondingly fast millisecond time response.¹⁹ The array of eight cantilevers enabled multiple reactions to be probed simultaneously.^{10,12} To probe motor-specific forces, differential measurements^{10,12} were acquired using an in-situ reference cantilever, coated with a control sequence oligonucleotide, **ref** (**ref**: HSC₆H₁₂-5'-TCT ATG CTG TTA CTC TGA CTC-3'), i.e., the bending of a cantilever tailored with the motor **X** was measured minus the bending of the in-situ reference cantilever, **ref**. Differential measurements were found to be critical since cantilevers can also respond to nonspecific influences such as temperature, reactions on the under side of the silicon cantilever, and nonfunctionalized sites of the gold film. However, motor-specific forces were deconvoluted by using a 21 mer oligonucleotide, which has the same length as the motor but cannot adopt the i-motif conformation. To ensure comparable oligonucleotide surface packing densities on each cantilever, both motor and reference oligonucleotides were immobilized in pH 9.0 buffer, whereby a random coil conformation is adopted. Initial studies found it necessary to optimize the motor surface packing density by the creation of mixed monolayers using mercaptoethanol “spacer” molecules. Extensive radiolabeling studies by Herne²⁰ and Steel²¹ using ³²P-probe DNA have shown that short alkanethiols remove nonspecifically adsorbed DNA from the gold surface, optimizing the density and the orientation of probe DNA molecules. Studies with ³²P-labeled complementary target DNA in solution have shown this procedure significantly improves the hybridization efficiency, which is typically less than 10% for pure DNA monolayers, to close to 100% for mixed monolayers.^{20,21} Hence, motor-coated surfaces

were subsequently incubated in a 1 mM mercaptoethanol for 1 h to remove nonspecifically adsorbed DNA, creating a reported^{20,21} packing density of $\sim 5.7 \times 10^{12}$ of **X**/cm².

The modified array was mounted in a sealed liquid chamber and the absolute deflection at the free end of each cantilever, Δz , was measured using a time-multiplexed optical detection system (Scentris, Veeco Instruments).^{10,12} The surface stress, which is defined as the reversible work per unit area, needed to stretch a preexisting surface, was calculated using the Stoney–Sader²² theory (eq 1). The difference in surface stress between the upper and lower sides of the cantilever, $\Delta\sigma$, is given by

$$\Delta\sigma = \frac{1}{K} \left(\frac{1}{3L} \right)^2 \frac{E}{1-\nu} \Delta z \quad (1)$$

where K is Sader’s correction factor (calculated²² to be 0.883), L is the length of the cantilever ($500\ \mu\text{m}$), t is the thickness ($1\ \mu\text{m}$), E is Young’s modulus (130 GPa), and ν is the Poisson ratio of silicon (0.28).

The surface stress forces generated by the open/close strokes of the molecular machine were studied, and cyclic operation probed the reversibility of the conformational change. The force exerted by a single motor was estimated on the basis of reported oligonucleotide surface density measurements using ³²P-radio-labeled DNA.^{20,21} Systematic investigation of the influence of the buffer environment provided new insight into the origin of the DNA-induced cantilever bending and facilitated tuneable micromechanical motion.

Results

The force exerted by surface-tethered DNA motors was investigated on microfabricated cantilevers using optical beam detection. The deflection of an array of eight cantilevers coated with either motor **X** or reference **ref** was monitored upon the injection of i-motif buffer (pH 5.0) and duplex buffer (pH 9.0). Typical absolute bending signals for **X**- and **ref**-coated cantilevers are shown in Figure 2a. At pH 9.0 both cantilevers behaved in a similar manner and showed a stable equilibrium signal under constant buffer flow. However, upon injection of pH 5.0 buffer, the response of the two cantilevers was found to be significantly different. Initially both cantilevers bent upward,

(19) Krecmer, P.; Moulin, A. M.; Stephenson, R. J.; Rayment, T.; Welland, M. E.; Elliott, S. R. *Science* **1997**, *277*, 1799–1802.

(20) Herne, T. M.; Tarlov, M. J. *J. Am. Chem. Soc.* **1997**, *119*, 8916–8920.

(21) Steel, A. B.; Levicky, R. L.; Herne, T. M.; Tarlov, M. J. *Biophys. J.* **2000**, *79*, 975–981.

(22) Sader, J. E. *J. Appl. Phys.* **2001**, *89*, 2911–2921.

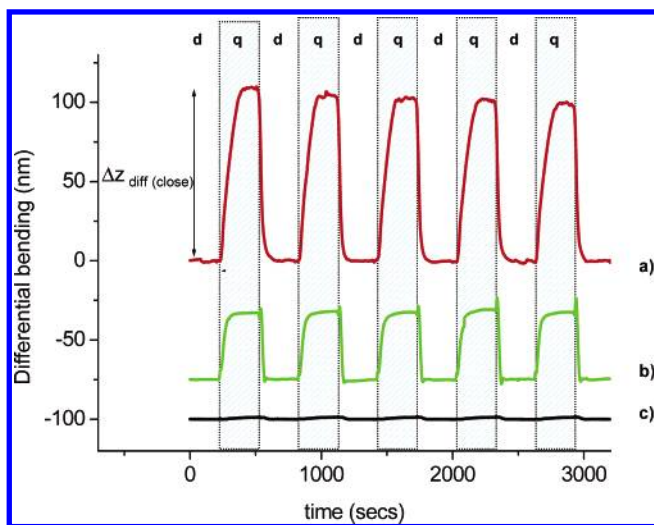


Figure 3. Differential cantilever bending measurements ($X - \text{ref}$) acquired during five successive cycles of the molecular machine. The pH of the buffer environment was alternately switched between i-motif forming pH 5.0 (the shaded regions, denoted q) and duplex-forming pH 9.0 (denoted d). The differential stress curves are offset on the y-axis to permit direct comparison of the magnitude of responses: (a) typical i-motif duplex induced cantilever differential response ($X_1 - \text{ref}_1$) in 0.1 M sodium phosphate buffer; (b) typical differential signal ($X_1 - \text{ref}_1$) of the i-motor in 0.1 M sodium phosphate buffer with an additional 1.0 M NaCl; (c) differential response between two reference DNA-coated cantilevers ($\text{ref}_2 - \text{ref}_1$) in 0.1 M sodium phosphate buffer with 0.1 M NaCl. Similar control sequence responses were observed in 0.1 M sodium phosphate buffer with 1.0 M NaCl.

which corresponded to a tensile surface stress, but subsequently the motor-coated cantilever exhibited a compressive stress associated with i-motif formation. In contrast the cantilever coated with the nonspecific reference oligonucleotide, ref generated a tensile stress at pH 5.0. This nonspecific response was attributed to changes in refractive index, temperature, drift, and nonspecific reactions occurring on the oligonucleotide and nonfunctionalized sites of gold film or the silicon cantilever. These findings are consistent our previous studies and emphasize the importance of differential measurements.^{10,12} Upon injection of duplex-forming pH 9.0 buffer, both the motor- and reference-coated cantilever signals were observed to return to the stable zero stress baseline.

The differential measurement ($X_1 - \text{ref}_1$), shown in Figure 2b, revealed the surface forces induced by specific duplex to i-motif conformational change. The differential signal in pH 9.0 gave a stable baseline but upon switching from the duplex to the i-motif conformation in pH 5.0 buffer, the bending signal was observed to increase to reach a stable equilibrium value under constant buffer flow, $\Delta z_{\text{diff(close)}}$ $\sim 110 \pm 9$ nm. This bending signal corresponded to a compressive surface stress change, $\Delta \sigma_{\text{diff(close)}}$ $\sim 33 \pm 3$ mN/m. Upon switching back to duplex buffer (pH 9.0), the direction of bending motion was reversed and the signal returned to the baseline value. The conversion from the i-motif to the duplex thus exerted $\Delta z_{\text{diff(open)}}$ $\sim 108 \pm 6$ nm, which corresponds to a differential tensile stress change $\Delta \sigma_{\text{diff(open)}}$ $\sim 32 \pm 2$ mN/m. The observed equivalent magnitude of open and close strokes reflects the reversibility of biomotor-induced cantilever actuation.

Five successive cycles of the molecular machine, shown in Figure 3a, generated an average $\Delta \sigma_{\text{diff(close)}}$ $\sim 33 \pm 3$ mN/m with no significant deterioration of motor activity over more than

20 cycles. The highly reversible, cyclic output of the molecular machine is in agreement with our previously reported solution-phase fluorescence and CD measurements.⁴ Evidently, the accumulation of “waste products” (H_2O and NaCl) does not interfere with the molecular mechanism of this machine. The differential signal between two levers coated with the same reference sequence ($\text{ref}_2 - \text{ref}_1$), shown in black in Figure 3c, was found to show no significant response to buffer pH and served as an important internal control to demonstrate the specificity of motor-induced cantilever bending.

The amplitude of the motor-fueled cantilever motion was investigated as a function of sodium phosphate buffer ionic strength and pH. The motor-induced cantilever bending signal acquired in two different buffers can be seen in Figure 3a,b. Over five cycles on the cantilever array, an average $\Delta z_{\text{diff(close)}}$ $\sim 100 \pm 9$ nm was measured in 0.1 M buffer, whereas a signal of $\sim 43 \pm 5$ nm was observed when 1.0 M NaCl was added to the phosphate buffer. The relative distribution of forces acquired in the two different buffers is shown in the histogram in Figure 4a.

The pH dependence of motor-induced micromechanical work was investigated at pH 5, 6, 7, 8, and 9 (0.1 M NaCl). Alternate injections of pH 5.0 buffer, followed by buffers with increasing pH served as another important control experiment. The normalized data shown in Figure 4b revealed a characteristic sigmoidal pH titration curve. Low surface stresses were observed at pH 5 and pH 6, but upon increasing the buffer pH a sharp transition was observed at approximately pH 6.7, reaching a maximum bending signal at pH 7.5. A small rise in stress was observed upon further increases in buffer pH up to pH 9.

Discussion

The findings reported herein show that the structurally defined duplex to i-motif conformational change induces in-plane nanomechanical surface stress on the microfabricated cantilever beam. Differential measurements acquired with an in-situ reference cantilever coated with an oligonucleotide, which cannot adopt the i-motif structure, were found to be essential. The hybrid device, triggered by biomolecular recognition, is environmentally “clean”, generating only salt and water byproducts enabling highly reversible, cyclic operation.

On the basis of reported radiolabeling studies,^{20,21} the motor surface packing density in a mixed monolayer was estimated to be $\sim 5.7 \times 10^{12}$ of X/cm^2 . Therefore, given the surface area of one side of the cantilever is 5×10^{-8} m^2 , the number of motors tethered to a single cantilever, n , is approximately 3×10^9 . This translates to a single motor footprint of 20 nm^2 . Assuming that each motor acts independently, the surface stress exerted by the stroke of a single molecular machine, s_x , is determined as follows:

$$s_x = \Delta \sigma_{\text{diff(open)}}/n \quad (2)$$

and estimated to be 11×10^{-12} N/m. It should be noted that this approximation of packing density is based on reported radiolabeling data^{20,21} and does not consider the true surface morphology and inherent roughness of gold but only the geometry of the cantilever. However, at present we cannot rule out possible contributions from less than 100% i-motif–duplex interconversion on the cantilever surface, so the efficiency of the nanomachine may be considerably higher. The

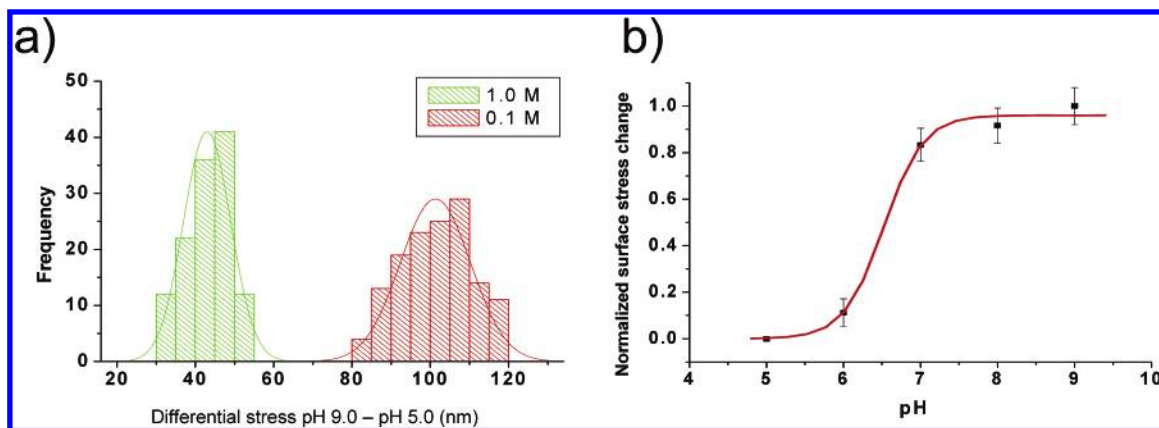


Figure 4. Manipulating the amplitude of micromechanical motion via buffer environment. (a) Histograms to show the change in cantilever bending upon conversion between the duplex and i-motif conformation $\Delta z_{\text{diff(close)}}(\mathbf{X}_1 - \mathbf{ref}_1)$ as a function of buffer ionic strength buffers. The distributions of differential measurements between pH 5.0 and pH 9.0, acquired in 0.1 M sodium phosphate buffer, 0.1 M NaCl (red) and those acquired in 0.1 M sodium phosphate buffer with 1.0 M NaCl (green), are shown. (b) Plot of the normalized change in surface stress, $\Delta z_{\text{diff(close)}}$, versus buffer pH in constant ionic strength 0.1 M sodium phosphate buffer. The differential data have been normalized to the value obtained for the conversion from pH 5.0 to pH 9.0 buffer.

deformation of the cantilever induced by an ensemble of DNA motors corresponds to a change in elastic energy of the mesoscopic beam of ~ 1 aJ ($E_{\text{elastic}} = -0.5 \times k \times \Delta z^2$), or alternatively an end-point loading actuation force of approximately 2 nN.^{10,12} The ability to manipulate both the direction and amplitude of an array of autonomous cantilever sensors offers considerable potential for micromechanical machinery, including valves, switches, and actuators triggered by molecular shape. It is envisioned that complex integrated nanomachines and high-throughput screening technology may be created via arrays of more than 1000 micromechanical cantilever beams,²³ with integrated electronic read-out,^{13,24,25} each functionalized with a different biomolecule by inkjet printing.²⁶ The plethora of molecular structures which could be exploited extends to DNA hairpins and multistranded structures to peptide nucleic acids and RNA aptamers.²⁷

The magnitude of surface stress associated with the i-motif motor, ~ 32 mN/m, is more than 10 times larger than our previous studies of classical hybridization of 12 mers, which generated a compressive surface stress of only ~ 2.3 mN/m.^{10,12} This suggests that conformationally induced stress may also provide a novel mechanism to further enhance the sensitivity of cantilevers toward picomolar concentrations of target DNA for applications as a label-free genomic sensor.^{10–14} However the fundamental origins of the nanomechanical stress induced by DNA hybridization reactions on cantilevers remains the subject of much interest and discussion in the literature.^{10–14} We previously reported that classical hybridization studies are highly sensitive to the oligonucleotide immobilization procedure and postulated that steric and electrostatic repulsion between oligonucleotides play an important role in the generation of a compressive surface stress.^{10,12} To rationalize the origin of the tensile surface stress associated with i-motif to duplex formation,

the steric geometry, and surface charge will be considered in the following discussion.

The influence of steric factors associated with duplex to i-motif conformational change is dependent on the motor surface packing density. Mixed monolayers of thiolated DNA with short alkanethiol spacers, are known to optimize hybridization efficiency by removing nonspecifically adsorbed DNA. This creates a significantly lower packing density than for cantilevers coated with pure DNA, as used in our previous cantilever hybridization experiments, which have a reported density^{10,12,20,21} of 1.3×10^{13} DNA molecules/cm², which translates to a single molecule footprint of ~ 3 nm². Furthermore, the theoretical 5.0 nm linear extension of each motor occurs perpendicular to the plane of the cantilever, and X-ray crystal structures of the i-motif and duplex structures report comparable, maximum lateral cross-sectional diameters of 1.9 and 2.0 nm, respectively.^{28,29} Indeed, the crystal structures of the i-motif reveal a “flat lath-shaped molecule”,^{28,29} with a pair of wide grooves and a pair of narrow grooves and the shortest separation between phosphate–phosphate duplexes across the narrow grooves of only 0.5 nm. Therefore, the repulsive compressive surface stress generated by the duplex to i-motif conformational change cannot be rationalized by simple geometric, steric considerations. Instead the significant influence of the buffer environment reported herein suggests that electrostatic forces play a prominent role in motor-induced surface stress generation. The sharp transition in stress observed at pH 6.7 is in close agreement with the reported solution-phase pK_a 6.5 for i-motif DNA.¹⁷ The surface pK_a is expected to depend strongly on the surface packing density,³⁰ and previous studies have reported a marked shift in the surface pK_a toward higher pH compared to solution phase studies. Cantilever stress measurements in 1.0 M NaCl sodium phosphate buffer showed significantly reduced stress signals compared to 0.1 M NaCl sodium phosphate buffer, which also indicates that electrostatic forces play an important role.

(23) Lutwyche, M. I.; Despont, M.; Drechsler, U.; Durig, U.; Haberle, W.; Rothuizen, H.; Stutz, R.; Widmer, R.; Binnig, G. K.; Vettiger, P. *Appl. Phys. Lett.* **2000**, *20*, 3299–3301.

(24) Calleja, M.; Tamayo, J.; Johansson, A.; Rasmussen, P.; Lechuga, L.; Boisen, A. *Sensor Lett.* **2004**, *1*, 1–5.

(25) Hafizovic, S.; Barrettino, D.; Volden, T.; Sedivy, J.; Kirstein, K.-U.; Brand, O.; Hierlemann, A. *Proc. Natl. Acad. Sci. U.S.A.* **2004**, *101*, 17013–17015.

(26) Bietsch, A.; Zhang, J.; Hegner, M.; Lang, H. P.; Gerber, Ch. *Nanotechnology* **2004**, *15*, 873–880.

(27) Savran, C. A.; Knudsen, S. M.; Ellington, A. D.; Manalis, S. R. *Anal. Chem.* **2004**, *76*, 3194–3198.

(28) Stokes, A. R.; Wilson, H. R. *Nature* **1953**, *171*, 738–740.

(29) Kang, C.; Berger, I.; Lockshin, C.; Ratliff, R.; Moyzis, R.; Rich, A. *Proc. Natl. Acad. Sci. U.S.A.* **1994**, *91*, 11636–11640.

(30) Fritz, J.; Baller, M. K.; Lang, H. P.; Strunz, T.; Meyer, E.; Guentherodt, H. J.; Delamarque, E.; Gerber, Ch.; Gimzewski, J. K. *Langmuir* **2000**, *16*, 9694–9696.

We postulate that, upon formation of i-motif DNA, the close proximity of four negatively charged phosphate backbones give rise to both intramolecular electrostatic repulsion between charged residues on a single i-motif and intermolecular repulsion between neighboring motors. A compressive stress therefore drives the bending of the cantilever downward (away from the gold surface) to increase the available surface area. In contrast, upon conversion to the duplex, intra- and intermolecular electrostatic repulsion may be relieved, causing the cantilever to bend upward. A simple electrostatic model predicts that, upon increasing ionic strength from 0.1 to 1.0 M, the Debye length between surface charge and counterion in solution is typically reduced from 10 to 0.1 nm, respectively.³¹ Therefore, one might expect increased charge screening will reduce electrostatic repulsion in the plane of the monolayer, which is in agreement with the experimental data shown in Figure 3 and Figure 4. However, our findings show that significant surface stress was observed in the presence 1.0 M NaCl buffer environment, where electrostatic forces are expected to be screened. This indicates that additional factors are contributing to surface stress including entropic, hydrophobic, hydration, and solvation surface forces.³¹ Water molecules are known to play an important role in the stabilization of the i-motif.^{27,28} The role of specific buffer anions and cations on motor-induced surface stress may also be significant. Future work will further investigate the origin of surface stress, including the role of the solvent, the influence of molecular entropy via temperature-dependent measurements,¹¹ the kinetics of conformational change using electrochemical triggers,^{15,16} oligonucleotide length, GC composition and 3' versus 5' immobilization.

Conclusion

In conclusion, we have demonstrated that the forces generated by duplex to i-motif conformational changes in a defined DNA system can be harnessed to perform micromechanical work on an array of silicon cantilevers. The direct integration of a dynamic biomolecular motor with cantilever arrays provides a way forward to a generation of “smart” bioinspired mechanical devices based on molecular concepts.

Experimental Section

Oligonucleotides. All oligonucleotides used herein were custom-synthesized by IBA GmbH, Germany.

Circular Dichroism Spectroscopy. The structures associated with the open and closed states in homogeneous solution were confirmed by CD spectroscopy.¹⁸ At pH 5.0 the closed state (nonthiolated **X/Y**, 1/1) has a CD spectrum which shows the distinct characteristics of i-motif DNA,⁴ with a strong positive band near 285 nm, a smaller negative band near 260 nm, and a crossover around 270 nm (Supporting Information). Examination of the open state at pH 9.0 by CD spectroscopy shows distinct characteristics of a B-form duplex DNA⁴ structure with a positive band near 275 nm, a negative band near 240 nm, and a crossover at 258 nm. In particular, the crossover at 258 nm rules out a random-coil structure.⁴

Cantilever Preparation. Cantilever arrays were purchased from Veeco Instruments and fabricated by IBM Research Laboratory, Ruschlikon, Switzerland (Figure 1b). Prior to functionalization, cantilevers were cleaned with piranha solution (1/1, 98% H₂SO₄ and 35% H₂O₂ for 10 min, followed by thorough rinsing in water (18.2 MΩ, Elga Maxima, Elga LabWater, Bucks, U.K.). Cantilever arrays were

coated on one-side with a thin film of gold (20 nm of Au with a 2 nm chromium adhesion layer, BOC Edwards Auto 500, U.K.; base pressure, 1×10^{-7} mbar; a thermal evaporation rate, 0.4 nm/s). Gold-coated cantilevers were then immediately inserted into glass microcapillary filled (Veeco Instruments) with thiolated **X** (2 μM **X** in a buffer containing 1 M NaCl and 0.1 M sodium phosphate buffer, pH 9.0) Using parallel microcapillaries,¹² four cantilevers could be coated with **X** and four with the control oligonucleotide **ref**. The entire array was subsequently immersed in 1 mM 2-mercaptoethanol (Sigma Aldrich) for 1 h, to remove nonspecifically adsorbed DNA.^{20,21} Cantilevers were then rinsed in ethanol (Fluka), followed by water (18.2 M Ohms, Elga Maxima), dried with a stream of nitrogen, and stored at 4 °C.

Equimolar solutions of mono- and dibasic sodium phosphate solutions (Sigma Aldrich) were titrated to produce buffers ranging from pH 5.0 to pH 9.0 (0.1 M). The pH of each solution was measured using pH meter (Delta 340, Mettler-Toledo, Beaumont Leys Leicester, U.K.). To investigate the influence of increased ionic strength on surface stress, 1.0 M NaCl (Sigma Aldrich) was added to the 0.1 M sodium phosphate buffer. All solutions were filtered (0.2 μm filters, Millipore Co., Bedford, MA) and degassed prior to use.

Multiple Cantilever Array Nanomechanical Detection. The absolute bending of all eight cantilevers was monitored using the serial time-multiplexed optical beam method with a single position sensitive detector (Scentris, Veeco Instruments Inc., USA). The functionalized cantilever array was mounted in a sealed liquid chamber with a volume of approximately 80 μL. The efficient exchange of buffers in the liquid chamber was achieved with a home-built gravity flow microfluidics system. The complete exchange between two buffers in the liquid chamber was estimated to take 50 ± 7 s. Equilibrium differential cantilever bending signals were not found to be significantly dependent on the direction of flow or flow rates investigated in this study. All bending measurements were performed under a constant buffer flow rate of 200 ± 30 μL/min in a temperature-controlled cabinet at 25 ± 0.5 °C. Labview software (National Instruments, Austin, TX) was implemented to automate the alternate flow of different pH sodium phosphate buffers via a six-way valve (Serial MVP, Hamilton, Reno, NV).

The resonant frequencies of an array of eight silicon cantilevers were found to vary by less than ~1% in agreement with previous reports.^{10,12} The alignment of each light source onto the end of each cantilever was probed by heating the liquid chamber by 1 °C. All eight gold-coated cantilevers were found to bend downward due to the bimetallic effect, and the optical alignment error was minimized to less than 5% for both motor- and reference-coated cantilevers. The variation in the differential signal between cantilevers on different microarrays was found to be approximately 20% and attributed to optical alignment, differences in the mechanical properties of the cantilevers, gold film thickness/morphology, and oligonucleotide functionalization. The findings reported herein were acquired on an array of eight cantilevers coated with **X** and **ref**, and comparable motor-induced surface stress was observed on more than five different sets of cantilever arrays.

A positive absolute or differential bending signal ($+\Delta z_{\text{diff}}$) is defined to a compressive surface stress (i.e. the cantilever bends away from the gold surface, as shown in Figure 1d) whereas a negative signal ($-\Delta z_{\text{diff}}$) correlates to tensile stress. Differential measurements were found to be critical for probing the highly specific biochemical forces induced by DNA motors. The differential signal $\Delta\sigma_{\text{diff}}$ is defined as the bending of a cantilever coated with motor **X** minus the response of an in-situ reference cantilever tailored with the control sequence **ref**. Signals were analyzed off-line using commercial software (Origin 7.0, OriginLab Co., Northampton, MA). $\Delta z_{\text{diff(close)}}$ is defined as the change in differential bending signal upon switching from duplex to i-motif DNA, $\Delta z_{\text{diff(open)}}$ is the differential bending signal upon switching from i-motif to duplex DNA, and $\Delta\sigma_{\text{diff(open)}}$ is the corresponding change in surface stress, calculated via the Stoney–Sader equation²² (eq 1).

(31) Israelachvili, J. *Intermolecular Surface Forces*, 2nd ed.; Academic Press: New York, 1992.

Acknowledgment. We thank the Interdisciplinary Research Collaboration (IRC) for Nanotechnology (Cambridge, University College London and Bristol), the London Centre for Nanotechnology, BBSRC, and the Human Frontier Science Program (CK) for funding. R.A.McK. is a Dorothy Hodgkin Royal Society Research Fellow. We thank Christoph Gerber, Hans Peter Lang, and Martin Hegner (University of Basel) and Trevor Rayment (Cambridge Chemistry) for use of gold evaporation facilities, Dr. AshwinSeshia (Cambridge Engineering) and Prof. Mike Horton (UCL Medicine) for fruitful discussions and support.

Note Added after ASAP Publication: In the version published on the Internet November 8, 2005, there were acknowledgments missing. This has been corrected in the version published November 10, 2005, and in the print version.

Supporting Information Available: Solution-phase CD characterization studies of i-motif and duplex DNA. This material is available free of charge via the Internet at <http://pubs.acs.org>.

JA0554514